# Geophysical constraints on the properties of a subglacial lake in northwest Greenland

Ross Maguire,[1,2] Nicholas Schmerr,[1] Erin Pettit,[3] Kiya Riverman[3] Christyna Gardner,[4] Daniella Della-Giustina,[5] Brad Avenson,[6] Natalie Wagner,[7] Angela G. Marusiak,[1] Namrah Habib,[5] Juliette I. Broadbeck,[5] Veronica J. Bray,[5] Hop Bailey,[5]

[1]Department Geological Sciences, University of Maryland, College Park MD, 20742, USA
[2]Department of Earth and Planetary Sciences, University of New Mexico, Albuquerque NM, 87131, USA
[3]College of Earth, Ocean, and Atmospheric Sciences, Oregon State University, Corvallis OR, 97331-5503, USA
[4]Department of Geosciences, Utah State University, Logan UT, 84322-4505, USA
[5]Lunar and Planetary Laboratory, University of Arizona, Tucson AZ, 85721-0092, USA
[6]Silicon Audio Inc., Austin TX, USA
[7]Department of Geosciences, University of Alaska, Fairbanks AK, 99775, USA

*Correspondence to*: Ross Maguire (rmaguire@umd.edu)

15 **Abstract.** We report the first ground-based observations of a subglacial lake in Greenland, confirming previous work based on airborne radar data. Here, we perform an active source seismology and ground penetrating radar survey in northwest Greenland where Palmer et al. (2013) first proposed the presence of a subglacial lake. From reflections of both the lake top and lake bottom, we observe a subglacial lake underlying approximately 845 m of ice, and constrain its depth to be between $10-15$ m. Additionally, using previously reported estimates of the lake's lateral extent, we estimate the total volume of liquid
20 water to be 0.15 km$^3$ (0.15 Gt of water). Thermal and hydropotential modeling both suggest that the lake should not exist unless it either sits over a localized geothermal flux high or has high salinity due to significant evaporite source in the bedrock. Our study indicates that this field site in northwestern Greenland is a good candidate for future investigations aimed at understanding lake properties and origins or for direct lake sampling via drilling.

## 1 Introduction

25 There is mounting evidence that subglacial lake systems below the Antarctic and Greenland ice sheet play an important role in glacier dynamics and ice-sheet mass balance considerations. In Antarctica, the presence of subglacial lakes is suspected to promote ice flow by reducing basal shear stress (e.g., Bell et al., 2007), and periodic drainage events have been linked to accelerated ice flow in outlet glaciers and ice streams (e.g., Stearns et al., 2008; Siegfried et al., 2016). Similarly, in Greenland subglacial lake systems also provide a reservoir for the storage of surface or basal melt water, and hence may be an important,

30 but largely unknown, factor in global sea level change. Additionally, subglacial lakes are of interest due to their ability to harbor complex microorganisms adapted to extreme environments (Achberger et al., 2016; Campen et al., 2019; Vick-Majors et al., 2016) and for paleoenvironmental information contained in subglacial lake sediments (Bentley et al., 2011).

While the presence and nature of subglacial lakes underlying the Antarctic ice sheet has been studied for more than 50 years,
35  the existence of subglacial lakes below the Greenland ice sheet (GrIS) is a relatively recent discovery and comparatively little
is known about their properties and origin. Detection of subglacial lakes has relied on a variety of methods, including airborne
radio-echo sounding (RES) (Robin et al., 1970; Siegert et al., 1996; Langley et al., 2011; Palmer et al., 2013; Young et al.,
2016; Bowling et al., 2019) satellite altimetry measurements (Fricker et al., 2007; Palmer et al., 2015; Siegfried & Fricker,
2018; Willis et al., 2015), and active source seismic experiments (Horgan et al., 2012; Peters et al., 2008). Using these
40  techniques, approximately 400 subglacial lakes have been detected in Antarctica (Wright & Siegert, 2012), of which 124 are
considered "active" (Smith et al., 2009). In Greenland, subglacial lakes were first detected in RES data by Palmer et al. (2013),
who identified two small (roughly 10 km$^2$) flat regions of anomalously high basal reflectivity below the northwestern GrIS.
These features, named "L1" and "L2", were discovered below 757 m and 809 m of ice respectively. Recently, Bowling et al.
(2019) greatly expanded the inventory of subglacial lakes in Greenland to approximately 54 candidates based on a combination
45  of RES and satellite altimetry data. The new inventory shows that, in contrast to subglacial lakes in Antarctica which tend to
form under thick (> 4 km) warm-based ice in the continental interior, the majority of subglacial lakes in Greenland are found
under relatively thin (1 - 2 km) ice near the margins of the GrIS. Bowling et al. (2019) find that most subglacial lakes in
Greenland appear to be stable features, showing temporally consistent RES signatures and an absence of vertical surface
deformation over the decadal time scales of observation. Of the 54 candidate lakes, only 2 showed signs of vertical surface
50  deformation indicative of active draining or recharge. While evidence of active subglacial lake dynamics in Greenland has
been sparse (Palmer et al., 2015; Willis et al., 2015), approximately 40% of Antarctic subglacial lakes appear to be active
features (Bowling et al., 2019).

The formation and location of the detected subglacial lake features in Greenland remains elusive because many are located in
55  regions where observations and modeling suggest that the base of the ice is frozen to its bed (MacGregor et al., 2016).
Complicating our understanding of the nature of subglacial lakes is the fact that uniquely identifying lakes in airborne radar
data is challenging since basal reflectivity is sensitive to both the physical properties and the roughness of the material
underlying the ice (e.g., Jordan et al., 2017). Amplitude anomalies of radar echoes in the range of +10 to +20 dB are often
interpreted as subglacial lakes, although flat regions of saturated sediment may produce similar anomalies. Furthermore, the
60  total volume of water stored in subglacial lake systems is unknown since airborne and space based remote sensing observations
are incapable of measuring lake depth (i.e., water column thickness). Seismic investigations provide an independent means of
confirming the presence of subglacial lakes and are capable of measuring lake depth and underlying geological structures
which can provide valuable clues into their formation and total volume.

65  In this study, we report results of an active source seismology and ground penetrating radar (GPR) survey performed in
northwestern Greenland (Figure 1), at the location where Palmer et al. (2013) first identified subglacial lake signatures in RES

data. Our survey was conducted above subglacial lake candidate L2 which is within the accumulation area of the ice sheet. Both seismic and GPR results show a flat reflector approximately 830 - 845 m below the surface, with a seismic reflection coefficient of -0.42 +/- 0.15, which is consistent with the acoustic impedance contrast between a layer of water below glacial

70 ice. Additionally, in the seismic data we observe an intermittent lake bottom reflection arriving between 14 - 20 ms after the lake top reflection, corresponding to a lake depth of approximately 10 - 15 m. Strong coda following the lake top and lake bottom reflections is consistent with a package of lake bottom sediments although its thickness and material properties are uncertain. Finally, we use these results to conduct a first-order assessment of the lake origins using a one-dimensional thermal model and hydropotential modeling based on published surface and bed topography (Morlighem et al., 2017). Because the

75 origins are still unclear, this site provides an intriguing opportunity for the first *in situ* sampling of a subglacial lake in Greenland, which could better constrain mechanisms of subglacial lake formation, evolution, and relative importance to glacial hydrology.

## 2 Methods

80 ### 2.1 Field experiment

In June 2018, we conducted a geophysical survey in northwestern Greenland above the candidate subglacial lake feature L2 (Palmer et al., 2013). This feature sits within a 980 km$^2$ drainage basin and is roughly adjacent (< 10 km) to the nearest drainage divide (Fig. 1A and 1B). The mean annual snow accumulation rate at the field site is ~30 cm/yr ice equivalent (determined from RACMO2 model results, Noël et al., 2018). In order to confirm the presence of the subglacial lake and investigate its

85 physical properties, we collected data using both active source seismology and GPR. The active source seismic experiment consisted of a moving line of 24 40 Hz vertical component geophones spaced 5 m apart. For each line, we collected data at 4 shot locations using an 8 kg sledgehammer impacted against a 1.5 cm thick steel plate. At each source location at least 5 hammer shots were stacked into a single shot gather in order to increase the signal to noise ratio. The first shot location of each line was offset 115 m from the first geophone, and subsequent shot locations were moved 115 m along the line. After data was

90 collected for each of the 4 shot locations, the line was moved 230 m east along the traverse and data collection was repeated. The seismic line was moved a total of 10 times, totalling 40 separate shot locations. Using this geometry, we obtained reflection points at the ice bottom spaced every 2.5 m along a traverse totalling 2400 m (Fig. 1C and 1D). The GPR survey was conducted across a ~5.5 km transect roughly parallel to the seismic survey (Fig. 1C), using a 10 MHz monopulse radar system.

95 ### 2.2 Seismic and GPR imaging

We created a longitudinal seismic reflection image by bandpass filtering data between 100 - 200 Hz and applying a normal moveout (NMO) correction with a velocity of 3700 m/s, which was found to be the average velocity of the ice column from

NMO analysis of the primary bed reflection. High frequency spatial noise with wavenumber greater than 0.05 m$^{-1}$ was removed with f-k filtering. Shot gathers with offsets of −115 m and 230 m from the first geophone contained an air wave arrival that

100    was muted by zeroing a 10 ms window with a moveout of 315 m/s. The seismic reflection profile (Fig. 2A) shows a clear ice bottom reflection across the entire transect arriving with a two-way travel time between 400 - 460 ms. The ice bottom multiple (i.e., a wave that has travelled twice between the surface and ice bottom) is also visible between 800 - 920 ms. From hereon, we refer to the ice bottom reflection as R1 and its multiple as R2. At transect distances between 0 - 1700 m, the R1 reflection is flat and relatively uniform in character, which we interpret to be the signal of the top of the subglacial lake. In this region,

105    R1 arrives at 457 ms, which corresponds to a depth of 845 m, assuming an average $V_P$ of 3700 m/s within the ice. At larger transect distances, the reflections arrive earlier with increasing distance, which likely reflects the bed topography adjacent to the subglacial lake. An additional reflection with opposite polarity of R1 is observed arriving between 14 – 20 ms after R1, which is consistent with a lake bottom reflection (Fig. 2B). This signal is intermittently observed but is most continuous at transect distances between 660 – 1200 m. The travel time differential between the lake top and lake bottom reflection is used

110    to measure the thickness of the water column across the seismic section. Assuming $V_P$ in the lake of 1498 m/s (Table 1), the lake is between 10 – 15 m deep (Fig. 2C). An uncertainty of +/- 50 m/s on lake velocity would correspond to a lake depth uncertainty of +/- 0.5 m. A strong coda following the lake bottom reflection is apparent which is likely caused by a thin (~ 10 m) sediment package underlying the lake (see Discussion).

115    To verify our seismic results, we also created a GPR image by converting the radar data to depth using a radar velocity of 172 m/μs (see Supporting Information). The subglacial lake is apparent as a flat reflector at an elevation of ~510 m across the majority of the transect (Fig. 3A). The surface topography slopes gently to the west across the transect, hence the lake is slightly deeper towards the east (Fig. 3B). The lake is beneath 840 m of ice at transect distances between 2 to 4.5 km, which roughly corresponds to the location of the seismic survey. The transition from the lake top to the adjacent bed is observed at

120    approximately 4100 m along the transect.

## 2.3 Basal reflectivity

In order to confirm that the flat region of R1 is consistent with a reflection from liquid water below ice, we calculate the reflection coefficient at the base of the ice by analysing the amplitudes of the first (R1) and second (R2) reflections. When

125    both R1 and R2 are visible, the basal reflection coefficient $c_R$ can be determined as a function of incidence angle $\theta$ using Eq. (1) where $A_{R1}$ and $A_{R2}$ are the amplitude of the first and second ice bottom reflections, respectively, $a$ is the absorption coefficient, and $L$ is the raypath length of the R1 reflection (e.g., Peters et al., 2008).

$$c_R(\theta) = 2 \frac{A_{R2}(\theta)}{A_{R1}(\theta)} e^{aL(\theta)}$$
(1)

At a given geophone, two factors control the amplitude ratio between R1 and R2. First, R1 and R2 reflect off of the lake with slightly different angles, which changes the relative amount of energy partitioned into each reflection. Second, since R2 travels
130   farther than R1, its amplitude is diminished due to geometrical spreading and attenuation. However, at incidence angles in this study, the difference in reflection coefficients between R1 and R2 is negligible. Additionally, the path lengths of R1 and R2 vary by < 5% between their shortest and farthest offsets. Therefore, to calculate the reflection coefficient $c_R$ we use the normal incidence approximation and compare amplitude ratios $A_{R2}/A_{R1}$ on individual seismograms. In order to minimize the influence of the air wave on $A_{R2}/A_{R1}$ ratio we exclude data from geophones with offsets between 135 – 155 m, where there is potential
135   interference between R1 and the air wave. Measurements of $A_{R1}$ and $A_{R2}$ are made prior to f-k filtering.

The relationship between the absorption coefficient $a$ and the seismic quality factor Q is given by Eq. (2), where $c$ is the seismic velocity, and $f$ is frequency (Bentley & Kohnen, 1976). While in principle, the spectral ratio of the R1 and R2 reflections can be used to determine the attenuation ($Q^{-1}$) of the glacial ice (Dasgupta & Clark, 1998; Peters et al., 2012) the low signal to
140   noise ratio of the R2 reflection prevents us from making a robust measurement. Here, we estimate the absorption coefficient $a$ based on the study of Peters et al. (2012), who reported Q = 355 +\- 75 in the upper 1 km of ice in Jakobshavn Isbrae, western Greenland. Using Eq. (2) with $c$ = 3.7 km/s, and assuming a frequency of 100 Hz (the predominant frequency observed in the reflections), this corresponds to an absorption factor a = 0.23 +/- 0.06.

$$Q^{-1} = \frac{ca}{\pi f}$$
(2)

Assuming an absorption factor of $a$ = 0.23, the average reflection coefficient of the lake bottom across the transect is -0.42 +/-
145   0.15 (Fig. 4A). In Fig. 4B, we plot $c_R$ calculated for each shot gather above the lake as a function distance along the transect. For comparison we show the expected reflection coefficients of several different geologic materials underlying glacial ice. The reflection coefficients were modeled using the two-term approximation of the Zoeppritz equations (e.g., Aki & Richards, 2002; Booth et al., 2015) with the material properties shown in Table 1. In contrast to other likely geological materials at the base of the ice, liquid water is expected to have a strongly negative reflection coefficient. The reflection coefficient modeled for
150   lithified sediments underlying ice is similar in amplitude to liquid water but opposite in sign, thus, without polarity information sedimentary rock strata could be mistaken for a lake signature. Here, we observe an opposite polarity of R1 and the seismic source which is consistent with the negative reflection coefficient expected for a subglacial lake. Thus, liquid water is the only material that is consistent with both the amplitude and sign of the observed reflections.

## 3 Discussion

### 3.1 Lake geometry and volume

If our interpretation of the observed reflections as signals from the lake top and bottom is correct, it implies that L2 could hold a significant volume of water. Assuming the imaged lake depth of approximately 15 m is representative of average lake depth throughout the roughly 10 km$^2$ surface area determined by RES, we estimate the total volume of liquid water to be 0.15 km$^3$ (0.15 Gt of water). While this is only a small fraction of the 217 +/- 32 Gt of ice that Greenland is estimated to lose each year to glacier discharge and surface melting (IMBIE Team Report, 2019), the net storage capacity of all of Greenland's subglacial lakes could be appreciable. To verify our interpretation of the lake top and bottom reflections, we modeled synthetic seismic waveforms of shot gather 12, which contained some of the clearest reflections. This shot gather corresponds to transect distances between 660 - 720 m in the seismic reflection image. Synthetic seismograms were computed using Specfem2D (Tromp et al., 2008) for two simple layered models of a 12 m thick lake underlying 850 m of glacial ice. In the first model the lake is underlain by a thick layer of sediments that extends to the bottom of the model domain. In the second model there is 10 m of sediments overlying a discontinuity with the bedrock below. The seismic velocity profiles for the two cases are shown in the insets in Fig. 5B and 5C. The source used in the simulations was a Ricker wavelet with a dominant frequency of 100 Hz. Fig. 5 shows a comparison between the observations and synthetics. In both the observed (Fig. 5A) and synthetic (Fig. 5B and 5C) shot gathers, the lake top and lake bottom reflections are separated by ~ 20 ms, and show a clear polarity reversal, which reflects the opposite sign of the acoustic impedance contrast between an ice-water and a water-lake bed transition. The observed shot gather contains a coda following the lake bottom reflection that is absent in the synthetics that do not include a discontinuity at the base of the sediment package (Fig. 5B). When a discontinuity between the sediment and underlying bedrock is included a strong sediment bottom reflection is introduced which more closely matches the observations (Fig. 5C). In the observed data it is difficult to clearly identify a sediment bottom reflection since the complex coda could be caused by reverberations within a thin sediment sequence, or many superposed reflections from individual discontinuities. However, if the first positive peak following the lake bottom reflection represents the base of the sediment, we can estimate a sediment thickness of 8.5 m assuming a sediment $V_P$ of 1700 m/s (Table 1).

### 3.2 Lake origin

While our results confirm that L2 is indeed a subglacial lake, its presence is perplexing given its location with a mean annual surface temperature of -22$^o$ C, and its position beneath a relatively thin column of glacial ice. In contrast to many well studied subglacial lakes below Antarctica such as Lake Vostok that lie below ~ 4 km of ice, the basal temperature at our field site is expected to be well below the pressure dependent melting point of ice. Distinguishing between the different hypotheses of subglacial lake formation has implications for the stability and dynamics of the GrIS since they predict different basal thermal and hydrological conditions. Thus, constraining the temperature of L2 is an important goal. We determine the range of possible basal temperatures using a 1D steady state advection-diffusion heat transfer model solved using the control volume method

(Patankar, 1980). The modeling assumes an ice density $\rho$ = 920 kg/m$^3$, a heat capacity $c_P$= 2000 J/kg/K, and a thermal conductivity $k$ = 2.3 W/m/K. The basal geothermal heat flux $q$ is varied between 50 – 60 mW/m$^2$, which is consistent with estimates derived from magnetic data (Martos et al., 2018) and thermal isostacy modeling (Artemieva, 2019). Fig. 6 shows results for surface temperatures T$_s$ of -20º C and -22º C and accumulation rate $w$ ranging from 0 to 0.3 m/yr ice equivalent.

190 When advection is ignored (i.e., no ice accumulation), most scenarios predict frozen bed conditions with the exception of the relatively warm surface condition (T$_s$ = $-20°$ C) and high heat flow ($q = 60$ mW/m$^2$) scenario (Fig. 6A). When ice accumulation is considered, all scenarios predict frozen bed conditions (Fig. 6B). For an ice accumulation rate of 0.3 m/yr, which most closely matches the conditions of the field site, the basal temperature is expected to be between approximately -12º C and -14º C.

195

There are several possible explanations for the existence of liquid water in L2, including hypersalinity, recharge by surface meltwater, high geothermal flux, and latent heat from freezing.

(1) Hypersalinity: If the lake is hypersaline it would depress the freezing temperature. Because the ice surrounding the lake
200 would be frozen to the bed, it would form a closed hydrologic system that could remain isolated on geologic timescales. In this scenario, the lake could represent a body of ancient marine water that was trapped as glacial ice advanced over the area and potentially further enriched in salt through cryogenic concentration processes (Lyons et al., 2005, 2019). Similar hypersaline lakes with salt concentrations several times higher than sea water are known to exist below the McMurdo Dry Valleys in Antarctica (Hubbard et al., 2004; Lyons et al., 2005, 2019; Mikucki et al., 2009) and in the Devon Ice Cap, Canada
205 (Rutishauser et al., 2018). However, because the current elevation of the lake is more than 500 m above sea level, it is unlikely to be trapped sea water as in the McMurdo Dry Valleys; however, we cannot rule out an ancient evaporite deposit as is proposed for the Devon Ice Cap (Rutishauser et al., 2018). However, the geologic map of Greenland does not indicate likely evaporites in this area (Dawes, 2004).

210 (2) Surface meltwater: The lake may be part of an open hydrological system that is continually recharged by surface meltwater. This lake, however, is in the accumulation area of the ice sheet, near the ice divide (Fig. 1B) and there are no obvious sources for significant surface recharge. To determine possible pathways for surface recharge, we estimate the local hydraulic head based on surface and bed elevations (Fig. S4) and find no pathways given the present resolution of bed and surface topography. It is possible that a subglacial pathway exists that is smaller than the resolution of BedMachine (Morlighem et al., 2017). If
215 the hydrological system is connected and the rate of recharge matches or exceeds the rate of freezing, a lake could persist despite sub-freezing temperatures in the lower part of the ice. At other locations in Greenland, observations of vertical surface deformation and collapse features have suggested that surface meltwater plays a prominent role in subglacial lake formation and dynamics (Palmer et al., 2015; Willis et al., 2015). Thus, subglacial lakes in Greenland could become more widespread as the GrIS responds to a warming polar climate.

220

(3) High geothermal flux. Anomalously high basal heat flux may promote melting of the GrIS from below (Fahnestock et al. 2001; Rogozhina et al., 2016). If this is the case, the local geothermal heat flux must greatly exceed regional estimates of the geothermal heat flux beneath the northwestern GrIS, which are typically in the range of 50 – 60 mW/m$^2$ (Artemieva, 2019; Martos et al., 2018; Rogozhina et al., 2016). Based on the one-dimensional model shown in Fig. 6, a geothermal flux on the

225  order of 100 mW/m$^2$ would be necessary to sustain the lake. While high heat flux in this region would be unexpected based on the cratonic bedrock geology and lack of recent volcanism, a local region of high heat flux could be promoted by the presence of upper crustal granitoids rich in radiogenic heat producing elements or hydrothermal fluid migration through pre-existing fault systems (e.g., Jordan et al., 2018).

230  (4) Latent heat from freezing. For either the isolated lake of actively freezing brine (as in Hypothesis 1) or the hydrologically connected continuous flow (Hypothesis 2), or if the lake is a relic of a larger freshwater body that is slowly freezing, the thermal profile of the ice would show a curvature change at depth due to a latent heat source at the bottom boundary. Given a latent heat of freezing of 334 J/g, freezing a layer 1 m thick to the bottom of the ice over one year is roughly equivalent to increasing the geothermal flux by 10 mW/m$^2$. Sustaining a freezing rate of several m/yr to generate the latent heat necessary

235  to maintain warm basal ice is less likely than locally elevated geothermal anomaly. We, therefore, rule out cryoconcentration and narrow the lake origin hypotheses to either anomalously high geothermal flux or hypersalinity due to local ancient evaporite. Measuring the thermal profile above this lake would provide important information to assess these hypotheses as the basal ice temperature would be near 0° C for the freshwater lake created by high geothermal flux hypothesis and substantially below zero for the hypersaline lake created by evaporite.

240

A freshwater lake and a hypersaline lake have different physical properties and thus may have different signatures that could be detected in geophysical surveys. Radar reflections from an ice/brine boundary undergoing freezing and cryoconcentration of the brine is known to cause scattering and decrease the reflectivity (Badgeley et al., 2017) which we do not see in our data; this provides a second justification to rule out cryoconcentration. Further, because the seismic velocity and density of water

245  depends on temperature and salinity, we would expect that lakes formed by different mechanisms would have slightly different basal reflection coefficients $c_R$. To estimate the difference in $c_R$ for different lake conditions, we calculate the basal reflectivity as described in Section 2.2 for low and high salinity end member scenarios. The $V_P$ in water is calculated as a function of pressure, temperature, and salinity using Equation (7) from Coppens (1981). At 0° C, the difference between $c_R$ of a freshwater lake and a saline lake with 100 ppt (approximately three times the salinity of ocean water) is 0.06 at normal incidence. While

250  a hypersaline lake could remain liquid at temperatures below 0° C, reducing temperature and increasing salinity have the opposite effect on seismic velocities thus reducing temperature below 0° C would decrease the contrast in $c_R$. Because the difference in reflection coefficient calculated for end member scenarios of 0.06 is smaller than the uncertainty on our measurements (approximately 0.15) we are unable to distinguish between different models of lake salinity and temperature

from our basal reflectivity analysis. On the other hand, because the electrical resistivity of water is strongly dependent on
255    salinity, magnetic sounding could provide useful constraints on lake composition. Future active source seismic experiments
focused on measuring Q within the overlying glacial ice could help us constrain the thermal profile above the lake (Peters et
al., 2012). Additionally, repeated seismic reflection or GPR surveys calculated along the same transect could provide clues
into whether or not lake levels are changing over time (e.g., Church et al., 2020). Direct sampling with drilling would provide
the best measurements on subglacial lake properties and could also yield useful biological and paleoenvironmental information.
260

## 4 Conclusions

We conducted an active source seismic reflection and GPR survey in northwestern Greenland above a site that was previously
identified as a possible subglacial lake. We observed a horizontal reflector at the base of the ice across the majority survey
with a seismic reflection coefficient of -0.42 +/- 0.15, confirming the presence of a subglacial lake. Additionally, we observed
265    a lake bottom reflection near the center of our seismic profile consistent with a lake depth of approximately 15 m. From
previous observations of the lateral extent of the lake based on RES (Peters et al. 2013), we estimate the subglacial lake holds
a total of 0.15 Gt of water. Strong coda arriving after the lake-bottom reflection suggests that the lake is underlain by a
sedimentary package but its thickness and material properties are uncertain. To the authors knowledge, this is the first time a
ground based geophysical survey has confirmed the existence of a subglacial lake in Greenland and provided constraints on
270    its depth. Understanding the nature and origins of recently detected subglacial lakes in Greenland is important since wet basal
conditions enable glacial ice to flow more easily which can further promote ice loss. Our analysis of the seismic, radar, as well
as thermal and hydropotential modeling narrow the lake origins to either locally high geothermal flux or an ancient evaporite
deposit. Future work, such as additional geophysical investigations or drilling expeditions, should focus on constraining the
temperature and salinity of the lake which will provide clues to its origin. Additionally, monitoring the vertical motion of the
275    ice surface above the subglacial lake system with satellite altimetry could provide further insight into the subglacial hydrology
(e.g., Siegfried & Fricker, 2018).

## Acknowledgements

Funding for this work was provided by the NASA Planetary Science and Technology Through Analog Research (PSTAR)
Grant Number 80NSSC17K0229. The authors thank SIIOS (Seismometer to Investigate Icy Ocean Worlds) team members
280    Chris Carr and Renee Weber for helpful discussions. Logistical support for field work in northwestern Greenland was provided
by Susan Detweiler.

# References

Achberger, A. M., Christner, B. C., Michaud, A. B., Priscu, J. C., Skidmore, M. L., Vick-Majors, T. J., & the WISSARD Science Team.: Microbial community structure of subglacial Lake Whillans, West Antarctica. *Front. Microbiol.*, *7*, 1–13. https://doi.org/10.3389/fmicb.2016.01457, 2016

Aki, K., & Richards, P. G.: *Quantitative seismology 2ⁿᵈ Ed.*, University Science Books, 2002

Artemieva, I. M.: Lithosphere thermal thickness and geothermal heat flux in Greenland from a new thermal isostasy method. *Earth-Sci. Rev.*, *188*(August 2018), 469–481. https://doi.org/10.1016/j.earscirev.2018.10.015, 2019

Badgeley, J. A., Pettit, E. C., Carr, C. G., Tulaczyk, S., Mikucki, J. A., & Lyons, W. B.: An englacial hydrologic system of brine within a cold glacier: Blood Falls, McMurdo Dry Valleys, Antarctica. *J. Glaciol.*, *63*(239), 387–400. https://doi.org/10.1017/jog.2017.16, 2017

Bell, R. E., Studinger, M., Shuman, C. A., Fahnestock, M. A., & Joughin, I.: Large subglacial lakes in East Antarctica at the onset of fast-flowing ice streams. *Nature*, *445*(7130), 904–907. https://doi.org/10.1038/nature05554, 2007

Bentley, C. R., & Kohnen, H.: Seismic refraction measurements of internal friction in Antarctic ice. *J. Geophys. Res.*, *81*(8), 1519–1526. https://doi.org/10.1029/jb081i008p01519, 1976

Bentley, M. J., Christoffersen, P., Hodgson, D. A., Smith, A. M., Tulaczyk, S., & Le Brocq, A. M.: Subglacial Lake Sediments and Sedimentary Processes: Potential Archives of Ice Sheet Evolution, Past Environmental Change, and the Presence Of Life. In *Antarctic Subglacial Aquatic Environments* (pp. 83–110). https://doi.org/10.1002/9781118670354.ch6, 2013

Booth, A. D., Emir, E., & Diez, A.: Approximations to seismic AVA responses: Validity and potential in glaciological applications. *Geophysics*, *81*(1), WA1–WA11. https://doi.org/10.1190/geo2015-0187.1, 2015

Bowling, J. S., Livingstone, S. J., Sole, A. J., & Chu, W.: Distribution and dynamics of Greenland subglacial lakes. *Nat. Commun.*, *10*(1), 1–11. https://doi.org/10.1038/s41467-019-10821-w, 2019

Campen, R., Kowalski, J., Lyons, W. B., Tulaczyk, S., Dachwald, B., Pettit, E., Welch., K.A., Mikucki, J. A.: Microbial diversity of an Antarctic subglacial community and high-resolution replicate sampling inform hydrological connectivity in a polar desert. *Environ. Microbiol.*, *21*(7), 2290–2306. https://doi.org/10.1111/1462-2920.14607, 2019

Church, G., Grab, M., Schmelzbach, C., Bauder, A., & Maurer, H.: Monitoring the seasonal changes of an englacial conduit network using repeated ground-penetrating radar measurements. *The Cryosphere*, *14*(10), 3269–3286. https://doi.org/10.5194/tc-14-3269-2020, 2020

Coppens, A. B.: Simple equations for the speed of sound in neptunian waters. *J. Acoust. Soc. Am.*, *69*(3), 862–863. https://doi.org/10.1121/1.385486, 1981

Dasgupta, R., & Clark, R. A.: Estimation of Q from surface seismic reflection data. *Geophysics*, *63*(6), 2120–2128. https://doi.org/10.1190/1.1444505, 1998

Dawes, P. R.: Explanatory notes to the geological map of Greenland, 1: 500 000, Humboldt Gletscher, Sheet 6. *Geological Survey of Denmark and Greenland (GEUS) Bulletin*, 1–48., 2004

315 Fahnestock, M., Abdalati, W., Joughin, I., Brozena, J., & Gogineni, P.: High geothermal heat flow, basal melt, and the origin of rapid ice flow in central Greenland. *Science*, *294*(5550), 2338–2342. https://doi.org/10.1126/science.1065370, 2001

Fricker, H. A., Scambos, T., Bindschadler, R., & Padman, L.: An Active Subglacial Water System in West Antarctica Mapped from Space. *Science*, *315*, 1544–1548. https://doi.org/10.1210/jcem-10-10-1361, 2007

Horgan, H. J., Anandakrishnan, S., Jacobel, R. W., Christianson, K., Alley, R. B., Heeszel, D. S., Picotti, S., Walter, J. I.:

320 Subglacial Lake Whillans - Seismic observations of a shallow active reservoir beneath a West Antarctic ice stream. *Earth Planet. Sc. Lett.*, *331–332*, 201–209. https://doi.org/10.1016/j.epsl.2012.02.023, 2012

Hubbard, A., Lawson, W., Anderson, B., Hubbard, B., & Blatter, H.: Evidence for subglacial ponding across Taylor Glacier, Dry Valleys, Antarctica. *Ann. Glaciol.*, *39*, 79–84. https://doi.org/10.3189/172756404781813970, 2004

Jordan, T. A., Martin, C., Ferraccioli, F., Matsuoka, K., Corr, H., Forsberg, R., Olesen, A., Siegert, M.: Anomalously high

325 geothermal flux near the South Pole. *Sci. Rep.*, *8*(1), 1–8. https://doi.org/10.1038/s41598-018-35182-0, 2018

Jordan, T. M., Cooper, M. A., Schroeder, D. M., Williams, C. N., Paden, J. D., Siegert, M. J., & Bamber, J. L.: Self-affine subglacial roughness: Consequences for radar scattering and basal water discrimination in northern Greenland. *The Cryosphere*, *11*(3), 1247–1264. https://doi.org/10.5194/tc-11-1247-2017, 2017

Langley, K., Kohler, J., Matsuoka, K., Sinisalo, A., Scambos, T., Neumann, T., Muto, A., Winther, J.-G., Albert, M.: Recovery

330 Lakes, East Antarctica: Radar assessment of sub-glacial water extent. *Geophys. Res. Lett.*, *38*(5), 1–5. https://doi.org/10.1029/2010GL046094, 2011

Lyons, W. B., Mikucki, J. A., German, L. A., Welch, K. A., Welch, S. A., Gardner, C. B., Tulaczyk, S. M., Pettit, E. C., Kowalski, J., Dachwald, B.: The Geochemistry of Englacial Brine From Taylor Glacier, Antarctica. *J. Geophys. Res.- Biogeo.*, *124*(3), 633–648. https://doi.org/10.1029/2018JG004411, 2019

335 Lyons, W. B., Welch, K. A., Snyder, G., Olesik, J., Graham, E. Y., Marion, G. M., & Poreda, R. J.: Halogen geochemistry of the McMurdo dry valleys lakes, Antarctica: Clues to the origin of solutes and lake evolution. *Geochim. Cosmochim. Ac.*, *69*(2), 305–323. https://doi.org/10.1016/j.gca.2004.06.040, 2005

MacGregor, J. A., Fahnestock, M. A., Catania, G. A., Aschwanden, A., Clow, G. D., Colgan, W. T., Gogineni, S. P., Morlighem, M., Nowicki, S. M. J., Paden, J. D., Price, S. F., Seroussi, H.: A synthesis of the basal thermal state of the

340 Greenland Ice Sheet. *J. Geophys. Res.-Earth*, *121*(7), 1328–1350. https://doi.org/10.1002/2015JF003803, 2016

Martos, Y. M., Jordan, T. A., Catalán, M., Jordan, T. M., Bamber, J. L., & Vaughan, D. G.: Geothermal Heat Flux Reveals the Iceland Hotspot Track Underneath Greenland. *Geophys. Res. Lett.*, *45*(16), 8214–8222. https://doi.org/10.1029/2018GL078289, 2018

Mikucki, J. A., Pearson, A., Johnston, D. T., Turchyn, A. V, Farquhar, J., Schrag, D. P., Anbar, A. D., Priscu, J. C., Lee, P.

345 A.: A Contemporary Microbially Maintained Subglacial Ferrous "Ocean." *Science*, *663*(5925), 397–401., 2009

Morlighem, M., Williams, C. N., Rignot, E., An, L., Arndt, J. E., Bamber, J. L., Catania, G., Chauche, N., Dowdeswell, J. A., Dorschel, B., Fenty, I., Hogan, K., Howat, I., Hubbard, A., Jakobsson, M., Jordan, T. M., Kjeldsen, K., K., Millan, R., Mayer, L., Mouginot, J., Noël, B. P. Y., O'Cofaigh, C., Palmer, S., Rysgaard, S., Seroussi, H., Siegert, M. J., Slabon, P.,

Straneo, F., van den Broeke, M. R., Weinrebe, W., Wood, M., Zinglersen, K. B.: BedMachine v3: Complete Bed
350  Topography and Ocean Bathymetry Mapping of Greenland From Multibeam Echo Sounding Combined With Mass
   Conservation. *Geophys. Res. Lett.*, *44*(21), 11,051-11,061. https://doi.org/10.1002/2017GL074954, 2017

Noël, B., van de Berg, W. J., van Wessem, J. M., van Meijgaard, E., van As, D., Lenaerts, J., Lhermitte, S., Munneke, P. K.,
   Smeets, C. J. P., van Ulft, L. H., van de Wal, R. S.: Modelling the climate and surface mass balance of polar ice sheets
   using RACMO2-Part 1: Greenland (1958-2016). *The Cryosphere*, *12*(3), 811–831., 2018

355 Palmer, S. J., Dowdeswell, J. A., Christoffersen, P., Young, D. A., Blankenship, D. D., Greenbaum, J. S., Benham, T., Bamber,
   J., Siegert, M. J.: Greenland subglacial lakes detected by radar. *Geophys. Res. Lett.*, *40*, 6154-6159.
   https://doi.org/10.1002/2013GL058383, 2013

Palmer, S. J., Mcmillan, M., & Morlighem, M.: Subglacial lake drainage detected beneath the Greenland ice sheet. *Nat.
   Commun.*, *6*. https://doi.org/10.1038/ncomms9408, 2015

360 Patankar, S. *Numerical heat transfer and fluid flow*. Taylor & Francis., 1980

Peters, L. E., Anandakrishnan, S., Alley, R. B., & Voigt, D. E.: Seismic attenuation in glacial ice: A proxy for englacial
   temperature. *J. Geophys. Res.-Earth*, *117*(2), 1–10. https://doi.org/10.1029/2011JF002201, 2012

Peters, L. E., Anandakrishnan, S., Holland, C. W., Horgan, H. J., Blankenship, D. D., & Voigt, D. E.: Seismic detection of a
   subglacial  lake  near  the  South  Pole,  Antarctica.  *Geophys.  Res.  Lett.*,  *35*(23),  1–5.
365  https://doi.org/10.1029/2008GL035704, 2008

Robin, G., Q., Swithinbank, C. W. M., & Smith, B. M. E.: Radio echo exploration of the Antarctic ice sheet. *International
   Symposium on Antarctic Glacial Exploration (ISAGE)*, *15*(86), 97--115. https://doi.org/10.1017/s0032247400061143,
   1970

Rogozhina, I., Petrunin, A. G., Vaughan, A. P. M., Steinberger, B., Johnson, J. V., Kaban, M. K., Calov, R., Rickers, F.,
370  Thomas, M., Koulakov, I.: Melting at the base of the Greenland ice sheet explained by Iceland hotspot history. *Nat
   Geosci.*, *9*(5), 366–369. https://doi.org/10.1038/ngeo2689, 2016

Rutishauser, A., Blankenship, D. D., Sharp, M., Skidmore, M. L., Greenbaum, J. S., Grima, C., Schroeder, D. M., Dowdeswell,
   J. A., Young, D. A.: Discovery of a hypersaline subglacial lake complex beneath Devon Ice Cap, Canadian Arctic.
   *Science Advances*, *4*(4), 1–7. https://doi.org/10.1126/sciadv.aar4353, 2018

375 Siegert, M. J., Dowdeswell, J. A., Gorman, M. R., & McIntyre, N. F.: An inventory of Antarctic sub-glacial lakes. *Antarct.
   Sci.*, *8*(3), 281–286. https://doi.org/10.1017/S0954102096000405, 1996

Siegfried, M. R., & Fricker, H. A.: Thirteen years of subglacial lake activity in Antarctica from multi-mission satellite
   altimetry. *Ann. Glaciol.*, *59*(76pt1), 42–55. https://doi.org/10.1017/aog.2017.36, 2018

Siegfried, M. R., Fricker, H. A., Carter, S. P., & Tulaczyk, S.: Episodic ice velocity fluctuations triggered by a subglacial flood
380  in West Antarctica. *Geophys. Res. Lett.*, *43*(6), 2640–2648. https://doi.org/10.1002/2016GL067758, 2016

Smith, B. E., Fricker, H. A., Joughin, I. R., & Tulaczyk, S.: An inventory of active subglacial lakes in Antarctica detected by
   ICESat (2003–2008). *J. Glaciol.*, *55*(192), 573–595. https://doi.org/10.3189/002214309789470879, 2009

Stearns, L. A., Smith, B. E., & Hamilton, G. S.: Increased flow speed on a large east antarctic outlet glacier caused by subglacial floods. *Nat. Geosci.*, *1*(12), 827–831. https://doi.org/10.1038/ngeo356, 2008

385  The IMBIE Team.: Mass balance of the Greenland Ice Sheet from 1992 to 2018. *Nature*. https://doi.org/10.1038/s41586-019-1855-2, 2019

Tromp, J., Komatitsch, D., & Liu, Q.: Spectral-element and adjoint methods in seismology. *Commun. Comput. Phys.*, *3*(1), 1–32., 2008

Vick-Majors, T. J., Mitchell, A. C., Achberger, A. M., Christner, B. C., Dore, J. E., Michaud, A. B., Mikucki, J. A., Purcell,

390      A. M., Skidmore, M. L., Priscu, J. C., & The WISSARD Science Team.: Physiological ecology of microorganisms in subglacial lake whillans. *Front. Microbiol.*, *7*(OCT), 1–16. https://doi.org/10.3389/fmicb.2016.01705, 2016

Willis, M. J., Herried, B. G., Bevis, M. G., & Bell, R. E.: Recharge of a subglacial lake by surface meltwater in northeast Greenland. *Nature*, *518*(7538), 223–227. https://doi.org/10.1038/nature14116, 2015

Wright, A., & Siegert, M.: A fourth inventory of Antarctic subglacial lakes. *Antarct. Sci.*, *24*(6), 659–664., 2012

395  Young, D. A., Schroeder, D. M., Blankenship, D. D., Kempf, S. D., & Quartini, E.: The distribution of basal water between Antarctic subglacial lakes from radar sounding. *Philos. T. R. Soc. A.*, *374*(2059). https://doi.org/10.1098/rsta.2014.0297, 2016

400
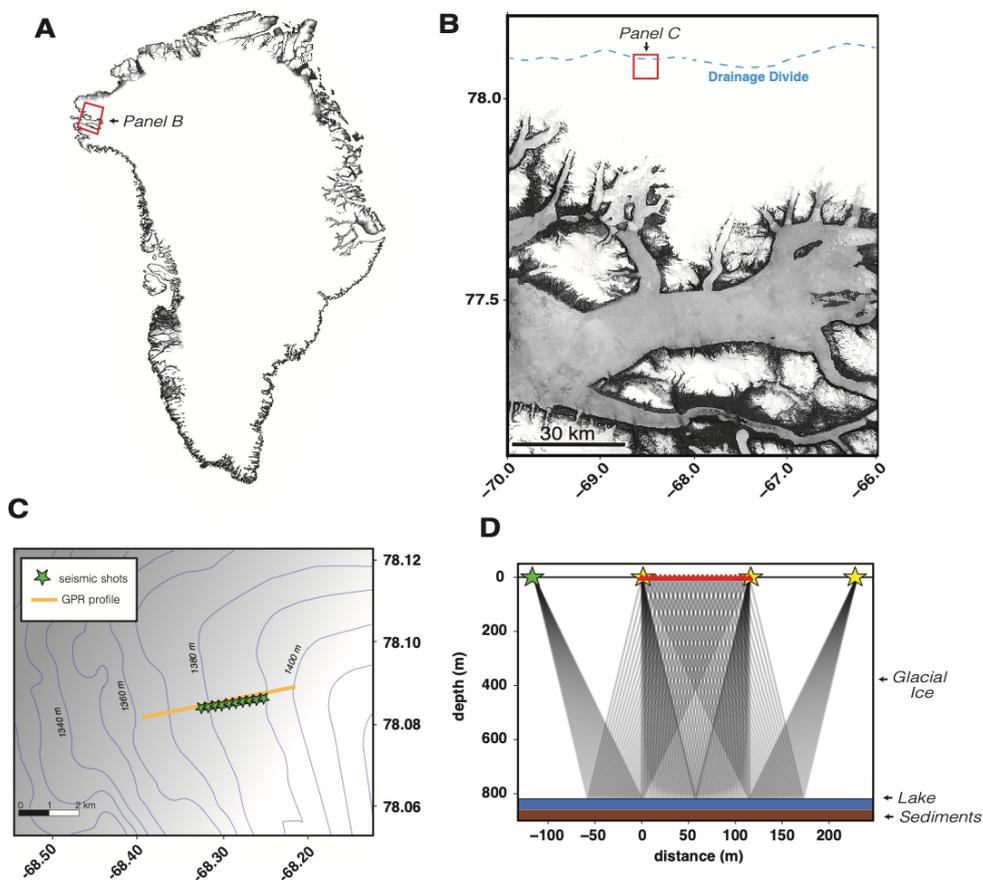
**Figure 1:** **(A) Map of Greenland showing our field location in the northwest. (B) Composite satellite image from Landsat 8 taken**
**between 2018-5-20 and 2018-5-27. (C) Close up map of field region. The green stars show the active source shot and the orange line**
**shows the track of the GPR survey. Only the first of 4 shot locations for each geophone line is plotted. (D) Geometry of the active**
**source experiment for a single geophone line. Raypaths of R1 are plotted for all 4 shot locations.**
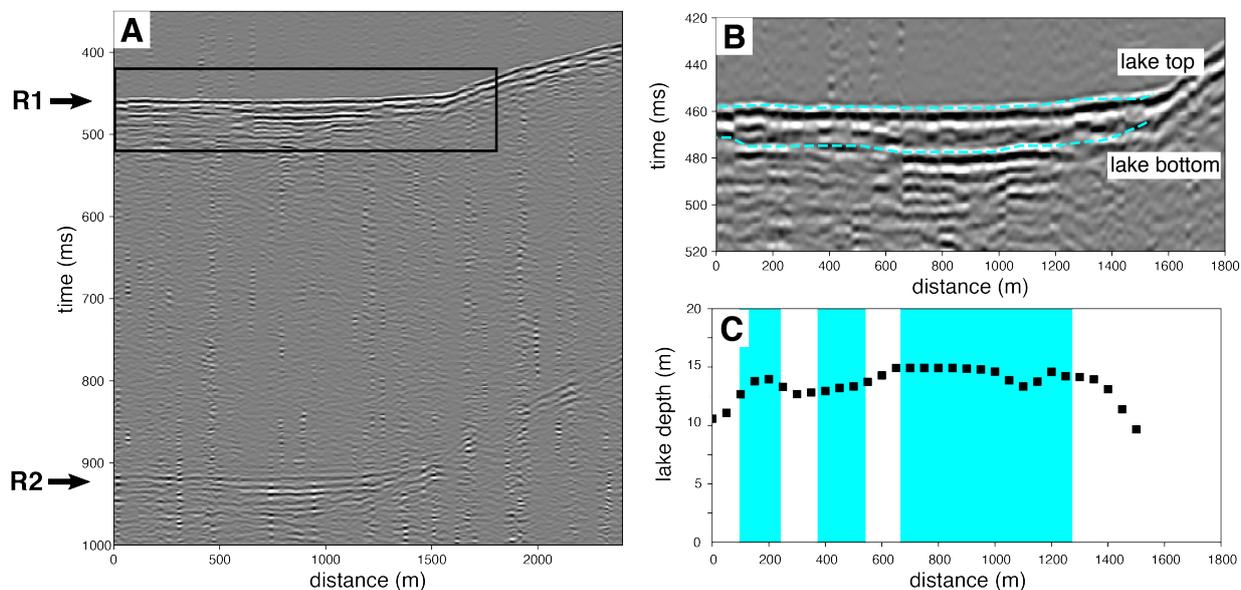
Figure 2. (A) shows the seismic reflection profile of the entire traverse. Reflections labeled R1 and R2 correspond to the primary reflection from the lake top and its multiple. A transect distance of 0 m corresponds to the southwestern end of the line. (B) shows a close up of the R1 reflection window (black rectangle in A), showing reflections from both the lake top and bottom. Travel time picks of the lake top and lake bottom reflections are drawn with the dashed blue line. The depth of the lake inferred from the picked reflections assuming a lake $V_P$ of 1498 m/s is shown in (C). Blue shaded regions indicate where the lake bottom reflection is most clearly identified.
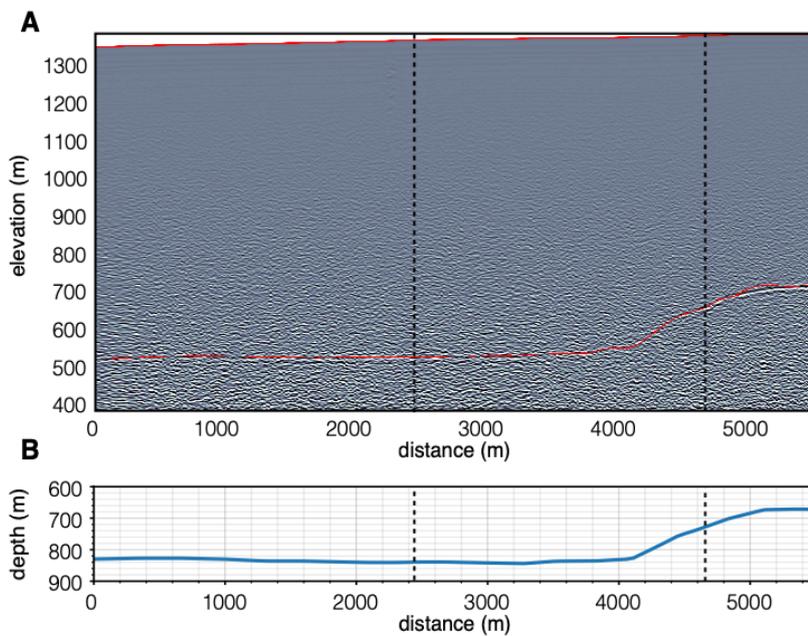
**Figure 3. GPR profile. (A) shows the 10 MHz radar data, unmigrated. The horizons outlined in red are the top and bottom of the ice. The depth from the surface to the base of the ice is shown in (B). Vertical dashed lines mark the approximate endpoints of the seismic survey.**

420

425
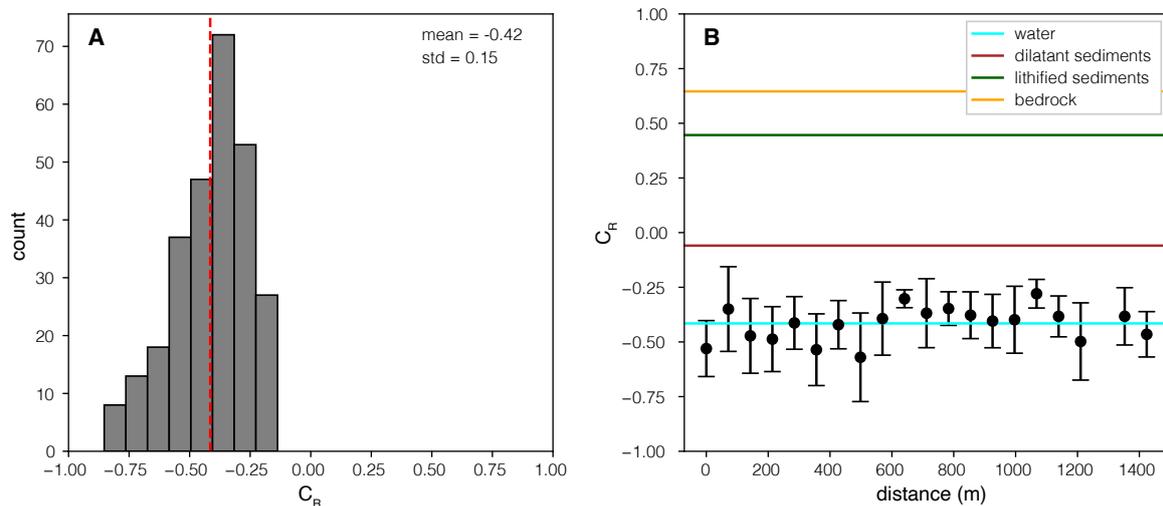
**Figure 4. (A) Distribution of reflection coefficients $c_R$ for locations where both R1 and R2 are observed. Only data collected over the subglacial lake is included. (B) Observed (black points) and expected (colored lines) reflection coefficients for shot gathers, shown as a function of distance along the transect.**
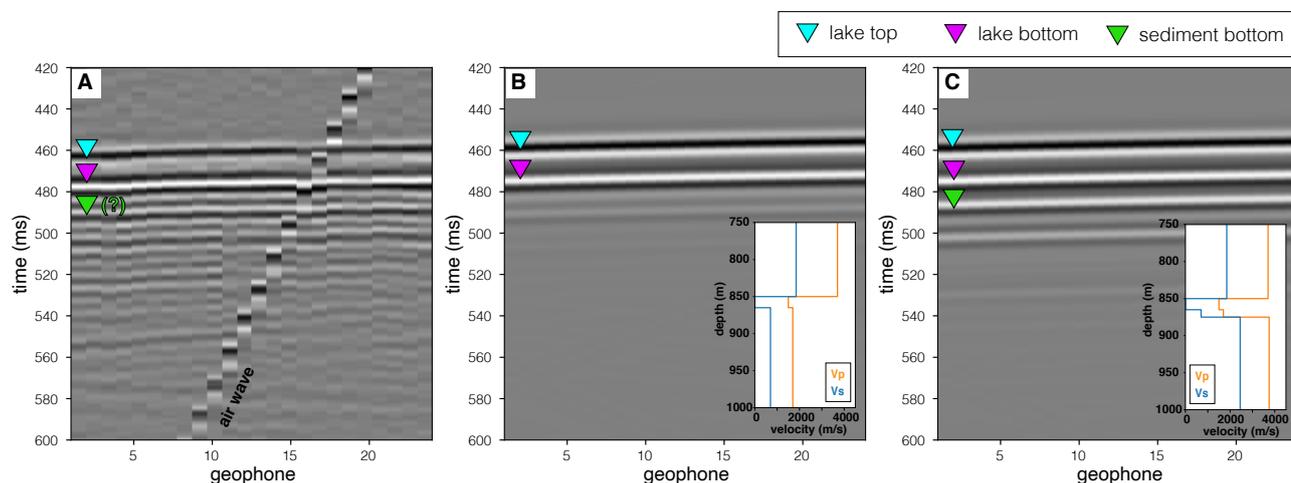
**Figure 5. Observed (A) and synthetic (B and C) seismic data for shot gather 12 bandpass filtered between 50 – 200 Hz. The offset from the source to geophone 1 is 230 m. The colored triangles indicate reflections from the lake top (blue), lake bottom (purple), and sediment bottom (green). The insets in panels B and C show the Vp and Vs models that were used to compute the synthetics. Both**
445 **models include a 12 m thick lake below 850 m of ice. The model used in (C) includes an additional discontinuity 10 m below the lake, which represents the boundary between the lake bottom sediments and underlying bedrock.**
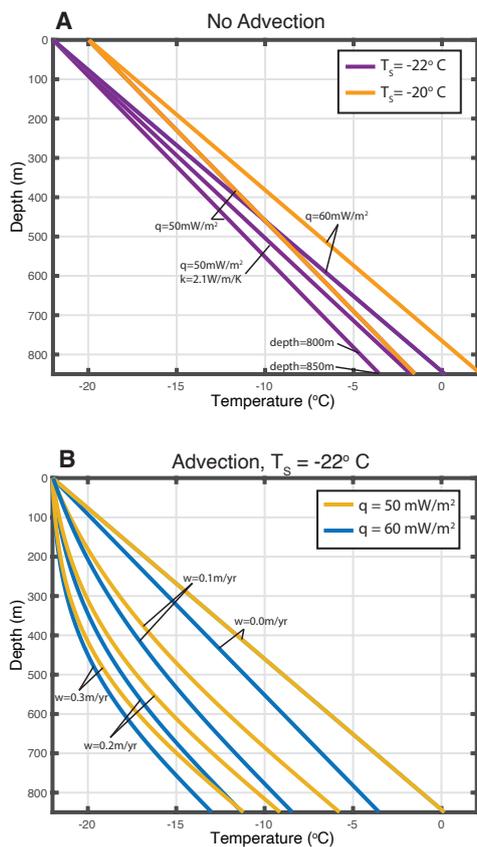
**Figure 6. Modeling of ice sheet thermal structure. Panel A shows thermal profiles neglecting advection for surface temperatures $T_S$**
450 **= -22° C and $T_S$ = -20° C. Panel B shows thermal profiles including advection for surface temperatures of $T_S$ = -22° C and $T_S$ = -20°**
**C, respectively. The basal heat flux q is varied between 50 – 60 mW/m² and the accumulation rate w is varied between 0 m/yr and**
**0.3 m/yr.**

| Material | $V_P$ (m/s) | $V_S$ (m/s) | Density (kg/m³) |
|---|---|---|---|
| Glacial ice | 3810 | 1860 | 920 |
| Water | 1498 | 0 | 1000 |
| Dilatant sediment | 1700 | 200 | 1800 |
| Lithified sediment | 3750 | 2450 | 2450 |
| Bedrock | 5200 | 2700 | 2700 |

**Table 1. Description of material properties used in reflection coefficient modeling. Values are from Peters et al. (2008).**
455